

## Measurements of heat flux in the atmospheric boundary layer by sodar and RASS: A first attempt

G. Peters, H. Hinzpeter, and G. Baumann

Meteorological Institute, University Hamburg, Hamburg, Federal Republic of Germany

(Received February 28, 1985; revised July 2, 1985; accepted July 2, 1985.)

By combined measurements with two ground-based remote sensing techniques, sodar and radioacoustic sounding system (RASS), the covariance of vertical wind and temperature perturbations can be determined. The estimation of errors indicates that this method is probably so accurate that profiles of the atmospheric turbulent heat flux can be determined. This is supported by experimental results.

### INTRODUCTION

The turbulent vertical heat flux plays an important role in many atmospheric processes. Its measurement is a delicate task, particularly if not only surface data but also vertical profiles are required. Therefore it is desirable to apply remote sensing techniques for this purpose.

One approach, which is based on the measurement of the vertical wind component variance by Doppler sodar, has been reported by *Weill et al.* [1980]. However, this method depends on the validity of rather restrictive assumptions regarding the status of the atmosphere.

The authors have not learnt of any attempt to derive the vertical heat flux  $Q$  remotely by the eddy correlation method:

$$Q = c_p \rho \langle T' w' \rangle \quad (1)$$

with

- $c_p$  specific heat at constant pressure;
- $\rho$  density;
- $T'$  temperature perturbation;
- $w'$  vertical wind component perturbation.

The vertical velocity  $w'$  can be determined by the well-known Doppler sodar technique, whereas no remote sensing system exists which yields  $T'$  with appropriate time and space resolution.

We will show that the flux  $\langle T' w' \rangle$  can nevertheless be obtained by a combined operation of sodar and RASS (radioacoustic sounding system). The RASS measures the sound velocity  $v$  relative to the sound-

ing system which is assumed to be at rest; thus  $v$  is the sum

$$v = c + w \quad (2)$$

where  $c$  is the speed of sound in a medium at rest and  $w$  is the component of the (Eulerian) advection velocity of the medium in the propagation direction of the sound beam;  $c$  can be determined by measuring  $v$  and  $w$  by RASS and sodar, respectively. The speed of sound  $c$  depends on the atmospheric temperature and humidity, and both effects on  $c$  are included almost exactly if the temperature is replaced by the virtual temperature. Thus, strictly speaking,  $c$  is a measure for the atmospheric enthalpy rather than for heat.

A sodar and RASS existing at the Hamburg Meteorological Institute have been operated simultaneously in order to determine  $w'$  and  $T'$ . It turned out that the straightforward calculation of the heat (enthalpy) flux according to (1) yields a strong downward bias. The variance of the sodar data, due to random errors, results in a large negative bias in the temperature-wind covariance. This bias is not a constant which could be calibrated in some way but is highly variable, depending on the actual sodar signal quality. However, it seems that this problem can be overcome by utilizing the entire covariance function instead of its value at zero time lag only. In this way, plausible heat flux values have been obtained. As a by-product the variance of the sodar random error can be estimated quantitatively as described below.

Both the sodar and the RASS technique are described elsewhere [e.g., *Brown and Hall*, 1978; *Frankel and Peterson*, 1976]. But for convenience a brief discussion of the systems employed here is given below.

Copyright 1985 by the American Geophysical Union.

Paper number 5S0545.  
0048-6604/85/005S-0545\$08.00

TABLE 1. Doppler Sodar System Parameters

| Parameter                               | Value               |
|---|---------------------|
| Transmit power (acoustic)               | 60 W                |
| Pulse width/range gate                  | 100 ms/17 m         |
| Pulse repetition period                 | 5 s                 |
| Acoustic frequency                      | 1675 Hz             |
| Antenna beam width (3 dB)               | $\pm 5^\circ$       |
| Averaging interval (in this experiment) | 15 s (three pulses) |

## THE REMOTE SENSING SYSTEM

### Doppler sodar

The Doppler sodar is a ground-based remote sensing system which transmits acoustic pulses into the atmosphere and receives the echo due to scattering at clear air microturbulent inhomogeneities. These scattering centers are considered as passive tracers which are advected with the local wind. Thus the Doppler shift of the received signal is a measure for the radial wind component in the scattering volume. Range resolution is achieved by gating of the received signal, a technique well known from radar application. In our case a monostatic, one-component system with a vertically directed antenna has been used. The mean system parameters are listed in Table 1.

The Doppler shift is derived from the frequency of the peak power density of the range-gated spectra averaged over a selected number of transmit pulses. Environmental noise recorded by the receiver causes deformation of the Doppler spectrum, resulting in a random error of the estimated peak frequency. This error is reduced by measurement of the background noise spectrum in advance of each transmit pulse and its subtraction from the signal spectra. In this way, noise sources with a persistence longer than the time delay between background measurement and the range-gated signals are suppressed. Therefore the decorrelation time of the remaining random wind error is shorter than one pulse period. This is an important assumption for the considerations below.

Environmental noise is not the only source of error, but normally it is the most important one; further effects which contribute to the shape of the Doppler spectrum have been discussed in the literature [Brown and Hall, 1978; Spizzichino, 1974]. The velocity signal  $w_S$  as measured by the sodar can be written as

$$w_S = w + r_S \quad (3)$$

where  $r_S$  is the random error.

### RASS

The RASS and its performance characteristics will be discussed in more detail, as this technique is not as widely used as the sodar. In addition the type of RASS which has been used for this experiment differs essentially from the radioacoustic sounding systems described by other authors.

The RASS concept is to operate an acoustic and an electromagnetic transmitter simultaneously at the same place. The compression and rarefaction of air characteristic to the acoustic field generate spatial variations of the refractive index which reflect some fraction of the electromagnetic energy. In contrast to the system used here, the shift of the peak frequency of the reflected signal spectrum relative to the transmit frequency is generally interpreted as a Doppler shift, which in turn is used as a measure for the sound velocity

$$v = -\omega_D/2k_e \quad (4)$$

where  $\omega_D$  is the frequency shift and  $k_e$  is the electromagnetic wave number. It has been shown by several authors that (4) holds only for a spectral width of the acoustic radiation which satisfies the condition

$$\Delta\omega \gg v/\Delta z \quad (5)$$

with  $\Delta\omega$  the spectral width of acoustic radiation and  $\Delta z$  the depth of the scattering volume.

More general expressions for the receiving spectrum are derived by Kon and Tatarskiy [1980], Kon [1981], Nalbandyan [1976a, b, 1977], and Peters et al. [1983]. Here only the consequences for the design of our RASS are summarized. In an atmosphere with turbulent flow the value of  $\Delta z$  is highly variable because of random deformations of the acoustic wave fronts. Therefore very high values of  $\Delta\omega$  are necessary in order to satisfy (5) reliably. This spectral spread of sound energy leads to a lack of the receiving signal as its intensity is proportional to the acoustic spectral density at the frequency  $\omega_a = \omega_D$ .

For very small values of  $\Delta\omega$ , i.e.,

$$\Delta\omega \ll v/\Delta z \quad (6)$$

we do not observe a Doppler shift according to (4) but rather a constant frequency shift equal to the acoustic transmit frequency  $\omega_a$ . A conventional RASS transmits acoustic pulses of finite width. In this case, conditions intermediate between (5) and (6) occur which yield receiving signal spectra having peaks somewhere between  $\omega_D$  and  $\omega_a$ . In order to avoid this ambiguity a RASS with continuous acous-

tic radiation of constant frequency ( $\Delta\omega = 0$ ) has been designed. Of course, no information about the sound speed  $v$  is contained in the observed frequency shift  $\omega_a$ . But the intensity of the received signal depends on  $v$ . If  $v$  satisfies the condition

$$v = \omega_a/2k_e \quad (7)$$

the signal intensity reaches a maximum. (This represents the well-known Bragg condition.) Therefore one possible way to determine  $v$  is to vary  $\omega_a$  (slowly) until a maximum receiving signal is observed. In our case, a fixed comb spectrum rather than a sweeping frequency has been used. Thus errors due to temporal variations of reflectivity during the sweeping are avoided. Range resolution is achieved by transmission of electromagnetic pulses. The essential system parameters of our RASS are listed in Table 2.

Measurements up to 1000 m altitude had been made with this system. This maximum level was not set by the general signal attenuation but by the horizontal wind causing a displacement  $D$  of the focus of the reflected energy at the ground.  $D$  can be estimated roughly as

$$D = 2UV^{-1}z \quad (8)$$

where  $z$  is the measuring height,  $U$  is the horizontal wind velocity averaged over  $z$ , and  $V$  is the sound velocity averaged over  $z$ . This is discussed in more detail, for example, by *Peters et al.* [1983]. In order to track the focus continuously over a larger distance, a 9-m parabolic dish had been used as an electromagnetic receiving antenna. Using (8), the maximum height range  $z_m$  for this RASS is

$$z_m/[\text{m}] = 1530\{U/[\text{m s}^{-1}]\}^{-1} \quad (9)$$

For example,  $U = 3$  m/s corresponds to about  $z_m = 500$  m. If higher range-wind products are required, the antenna has to be extended or some displacement device must be provided. For considerably higher measuring altitudes a lower sound frequency must be used in order to avoid excessive sound attenuation.

The sound absorption length  $\alpha$  increases approximately inversely proportional to the frequency and varies in a wide range depending on atmospheric humidity and temperature. For sound frequencies used in this RASS,  $\alpha$  can vary between 150 m and 700 m according to *Harris* [1967].

From now on the sound velocity signal as measured by RASS will be labeled as  $v_R = v + r_R$  where  $r_R$  is the random measuring error. Since the magnitude of  $r_R$  is important for assessing the feasibility of our application, comparisons with in situ tower measurements have been made in two ways:

If vertical sound beams are considered, values of  $v_R$ , averaged over 10 min, depend practically only on the local temperature (and humidity) as the mean vertical wind component is generally small in the atmospheric boundary layer. As an example the regression of RASS-derived temperatures versus in situ measurement at a tower at four height levels are shown in Figure 1 for a 20-hour time period. The influence of humidity on  $v$  has been taken into account by utilizing ground measurements of humidity and assuming that the mixing ratio  $\mu$  remains constant with height. ( $T = kv_R^2 - 0.516\mu$  with  $k = 2.488 \times 10^{-3} \text{ K s}^2/\text{m}^2$ .)

The scatter in the regression corresponds to a standard deviation  $\sigma(T) = 0.3 \text{ K}$  (or  $\sigma(v_R) = 18 \text{ cm/s}$ ) between tower and RASS data. It must be kept in mind that these differences are to be attributed partly

TABLE 2. Bragg-RASS System Parameters

| Parameter                                     | Value  |
|---|--|
| Acoustic reference frequency $x$              | 1250 Hz to 1400 Hz according to an environmental temperature range from approximately $-25^\circ\text{C}$ to $+35^\circ\text{C}$ |
| Peak frequencies of the acoustic spectrum     | $(x + i \times 5) \text{ Hz}$ , $i = 0-7$  |
| Acoustic power                                | 20 W   |
| Acoustic beam width (3 dB)                    | $\pm 6.5^\circ$  |
| Electromagnetic frequency                     | 593.5 MHz  |
| Electromagnetic power                         | 30 W   |
| Electromagnetic transmitter beam width (3 dB) | $\pm 8^\circ$  |
| Pulse repetition period                       | 2, 4, 8, 16 $\mu\text{s}$  |
| Duty cycle                                    | 1/16 (fixed)   |
| Range resolution (variable)                   | 19, 38, 75, 150 m  |
| Receiver aperture                             | 9-m diameter parabolic dish  |

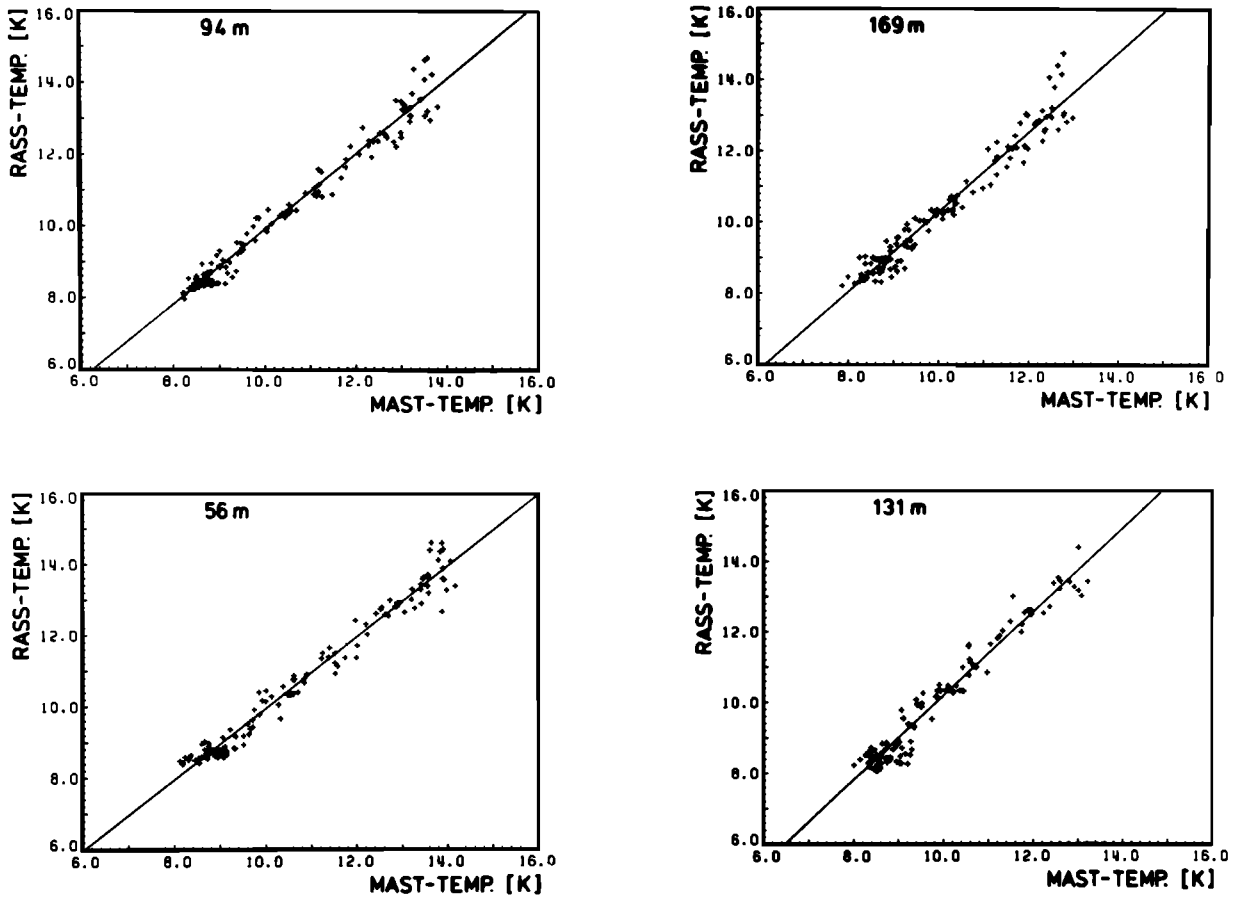


Fig. 1. RASS-derived temperature versus temperature as measured at an instrumented tower: 10-min averages of a 20-hour measuring period.

to the nonvanishing vertical wind component. Also, the horizontal distance between the tower position and the RASS (700 m) is responsible for some differences.

The second method to verify RASS data utilizes the fact that high-frequency variations ( $<10$  min) of  $v$  are primarily caused by variations of  $w$ . Only a small amount of the variance of  $v$  is due to temperature variations. Even in convective conditions the ratio of these contributions to the variance of  $v$  should not exceed  $10^{-1}$  [e.g., *Caughey et al.*, 1978]. Thus the standard deviation of  $v$  can be compared with the standard deviation of the wind component parallel to the sound beam. This had also been done at the same tower with vertical high-resolution propeller anemometers at three height levels. An example for a 24-hour measuring period is shown in Figure 2. For very weak turbulence (left lower corner of the regression plots) the data show a plateau indi-

cating a minimum standard deviation of the RASS somewhat less than 10 cm/s. This can be attributed to the system random measuring error. This figure refers to nearly instantaneous data (averaging interval 10 s). Consequently, an estimated error of  $\pm 5$  cm/s standard deviation seems to be realistic for longer averaging intervals.

#### THE METHOD TO DETERMINE $\langle w'T' \rangle$

In order to determine the sound velocity relative to the medium according to (2) by simultaneous operation of RASS and sodar we must consider three contributions to the measured sound velocity signal  $c_R = v_R - w_S = c + r_R - r_S$ : (1) temperature and humidity, (2) random error of the Doppler sodar  $r_S$ , and (3) random error of the RASS  $r_R$ .

It appears highly unlikely that the high-frequency variations of temperature and humidity could ever be

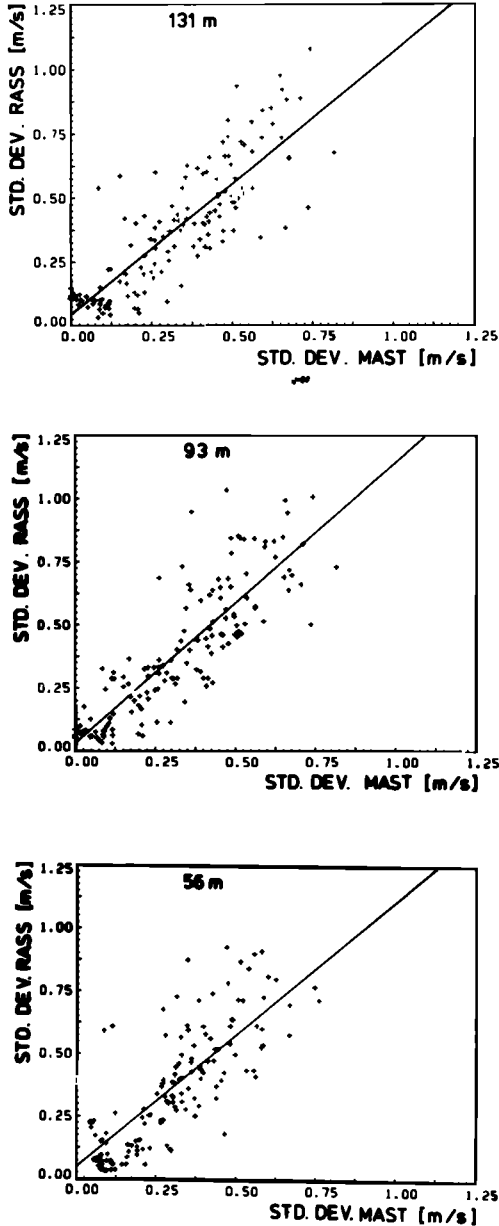


Fig. 2. Standard deviation of RASS-derived sound velocity versus standard deviation of high-resolution vertical propeller anemometers: 10-min averages of a 20-hour measuring period.

derived with sufficient accuracy in this way, since contributions 2 and 3 will generally dominate. Nevertheless, the heat flux can be determined, as will be shown below.

By straightforward correlation of RASS and sodar data we obtain the heat flux as

$$Q_m = c_p \rho \langle w'_s T'_R \rangle = c_p \rho \alpha \langle w'_s c'_R \rangle \quad (10)$$

or

$$q_m = \frac{Q_m}{c_p \rho \alpha} = \langle w'_s c'_R \rangle \quad (11)$$

with  $\alpha = 1.69 \text{ K m}^{-1} \text{ s}^{-1}$ . Here  $q_m$  is the sample mean of the function

$$x(i) = w'_s(i\tau)c'_R(i\tau) \quad i = 0, \pm 1, \pm 2, \pm 3, \dots \quad (12)$$

where  $\tau$  is one sampling increment (15 s in this case).

For further discussion we consider the function

$$x(i, j) = w'_s[(i - j)\tau]c'_R(i\tau) \quad (13)$$

which corresponds to

$$q_m(j) = \langle x(i, j) \rangle = \frac{1}{n} \sum_{i=i_0+1}^{i_0+n} x(i, j) \quad (14)$$

We see that  $q_m(j)$  is the sampled covariance function of  $w'_s$  and  $v'_R - w'_s$  and in particular

$$Q_m = c_p \rho \alpha q_m(0) \quad (15)$$

First we evaluate  $q_m(j)$  using the relations  $w'_s = w' + r_s$  and  $v'_R = v' + r_R$ :

$$q_m(j) = \langle w'_s(i - j)c'_R(i) \rangle \quad (16)$$

$$q_m(j) = \langle [w'(i - j) + r_s(i - j)][c'(i) + r_R(i) - r_s(i)] \rangle \quad (17)$$

For brevity of notation the primes will be omitted:

$$q_m(j) = \langle [w(i - j) + r_s(i - j)][c(i) + r_R(i) - r_s(i)] \rangle \quad (18)$$

For  $n \rightarrow \infty$  all terms with uncorrelated factors  $\langle w(i - j)r_R(i) \rangle$ ,  $\langle w(i - j)r_s(i) \rangle$ ,  $\langle r_s(i - j)c(i) \rangle$ ,  $\langle r_s(i - j)r_R(i) \rangle$  will vanish, and so

$$\lim_{n \rightarrow \infty} q_m(j) = \langle w(i - j)c(i) \rangle - \langle r_s(i - j)r_s(i) \rangle \quad (19)$$

As stated earlier, we may assume that the correlation time of the statistical error  $r_s$  is not longer than one sodar pulse period. Thus we may replace its sampled autocorrelation function by a delta function:

$$q_m(j) = \langle w(i - j)c(i) \rangle - \sigma^2(r_s)\delta(0, j) \quad (20)$$

We see that  $q_m(0)$  is not equal to the covariance of  $w$  and  $c$  but is biased by  $\sigma^2(r_s)$ , which can be very large.

Measurements of heat flux spectra under neutral and unstable conditions show [Panofsky and Mares, 1968] a spectral peak at approximately

$$f = 0.1U/z \quad (21)$$

where  $f$  is frequency,  $z$  is the measuring altitude, and  $U$  is the wind speed.

For higher frequencies the cospectra of  $w$  and  $T$  decrease fairly steeply as  $f^{-8/3}$ . From this we may conclude that the width of the covariance function

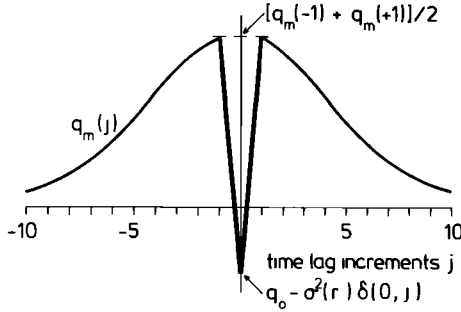


Fig. 3. Expected covariance function of the sodar-derived vertical wind velocity signals  $w'_s$  and the RASS-derived sound velocity signal corrected for the vertical wind  $v'_R - w'_s$ :  $\langle w(i-j)c(i) \rangle - \sigma^2(r_S)\delta(0, j)$ .

$\langle w(i-j)c(i) \rangle$  extends over several time lag increments if the condition

$$1/f \gg \tau \quad (22)$$

is satisfied. This means that  $\langle w(i-j)c(i) \rangle$  does not change very much with one time lag increment and we can replace the (not measurable) value  $\langle w(i)c(i) \rangle$  by an interpolated value. The simplest way is a linear interpolation between adjacent values

$$q(0) = [q_m(-1) + q_m(+1)]/2 \quad (23)$$

See Figure 3 for an illustration of the procedure.

Some further improvement could probably be achieved by fitting a suitable model function to the sampled covariance function, but for demonstration of the feasibility the simple interpolation scheme of (23) is adequate.

To estimate the accuracy of this measuring technique, we calculate the variance of the heat flux thus determined:

$$\begin{aligned} \sigma^2(Q) &= c_p^2 \rho^2 \alpha^2 \sigma^2[q(0)] \\ &= c_p^2 \rho^2 \alpha^2 \{ \sigma^2[q_m(-1)] + \sigma^2[q_m(+1)] \} / 2 \end{aligned} \quad (24)$$

where  $\sigma^2[q_m(j)]$  can be calculated according to *Jenkins and Watts* [1968]:

$$\begin{aligned} \sigma^2[q_m(j)] &= \sigma^2[\langle w_S(i-j)c_R(i) \rangle] \\ &= \frac{1}{n} \sum_{i=-\infty}^{\infty} \gamma_{w_S w_S}(i) \gamma_{c_R c_R}(i) + \gamma_{w_S c_R}(i+j) \gamma_{c_R w_S}(i-j) \end{aligned} \quad (25)$$

where  $\gamma_{w_S w_S}(k)$  and  $\gamma_{c_R c_R}(k)$  are the autocovariance functions of  $w_S$  and  $c_R$ , respectively, and  $\gamma_{w_S c_R}(k)$  is the cross-covariance function between  $w_S$  and  $c_R$ . Equation (25) holds if  $n$  is large against the decorrelation lags of the processes  $w_S$  and  $c_R$ . Substituting  $w_S = w + r_S$  and  $c_R = c + r_S - r_S$  in (23), keeping in

mind that  $r_S(i-j)$  is not correlated with  $r_S(i)$  for  $j \neq 0$  and assuming likewise that  $r_R(i-j)$  is not correlated with  $r_R(i)$  for  $j \neq 0$ , we obtain, for  $j = 0$ ,

$$\begin{aligned} \sigma^2[q_m(j)] &= \frac{1}{n} \left[ \sum_{i=-} (\gamma_{w_S w_S}(i) \gamma_{c_R c_R}(i) + \gamma_{w_S c_R}(i+j) \gamma_{c_R w_S}(i-j)) \right. \\ &+ \sigma^2(w) \sigma^2(r_R) + \sigma^2(w) \sigma^2(r_S) \\ &+ \sigma^2(c) \sigma^2(r_S) + \sigma^2(r_S) \sigma^2(r_R) \\ &\left. + \sigma^2(r_S) \sigma^2(r_S) - 2\gamma_{w_S c_R}(2j) \sigma^2(r_S) \right] \end{aligned} \quad (26)$$

Even for vanishing instrumental errors ( $\sigma(r_R) = \sigma(r_S) = 0$ ) the variance of  $q_m(j)$  is not zero because of the first term. This does not represent a measuring error but the range of variation of the heat flux which is compatible with statistical stationarity of the turbulence.

The estimated random error of  $q_m(j)$  due to the instrumental errors is given by the last six terms of (26) and will be designated  $\sigma(r_q)$ :

$$\begin{aligned} \sigma^2(r_q) &= \sigma^2(w) \sigma^2(r_R) + \sigma^2(w) \sigma^2(r_S) + \sigma^2(c) \sigma^2(r_S) \\ &+ \sigma^2(r_S) \sigma^2(r_R) + \sigma^2(r_S) \sigma^2(r_S) - 2\gamma_{w_S c_R}(2j) \sigma^2(r_S) \end{aligned} \quad (27)$$

As mentioned earlier and confirmed by measurements, the variability of  $v$  due to high-frequency temperature variations is generally small in comparison to the variability of the vertical wind component,

$$\sigma(c) \ll \sigma(w) \quad (28)$$

Therefore terms III and VI are small in comparison to term II and will be neglected. Further, we may assume that the random measuring error of the RASS is much smaller than that of the sodar because of the better signal quality of the RASS,

$$\sigma(r_R) \ll \sigma(r_S) \quad (29)$$

Thus only II and V remain, after neglecting IV and I. Since  $r_S$  and  $w$  are not correlated, and remembering  $w_S = w + r_S$ , we may write  $\sigma^2(w_S) = \sigma^2(r_S) + \sigma^2(w)$  and, to a first approximation,

$$\sigma^2(r_q) \approx \sigma^2(r_S) \sigma^2(w_S) \quad (30)$$

Thus the final expression for the random instrumental error of the heat flux is

$$\sigma(r_Q) = n^{-1/2} c_p \rho \alpha \sigma(r_S) \sigma(w_S) \quad (31)$$

Here,  $\sigma(r_S)$  can be estimated using (20) and (23):

$$\sigma(r_S) = [q(0) - q_m(0)]^{1/2} \quad (32)$$

Also,  $\sigma(w_S)$  can be derived from the time series of  $w_S$ ,

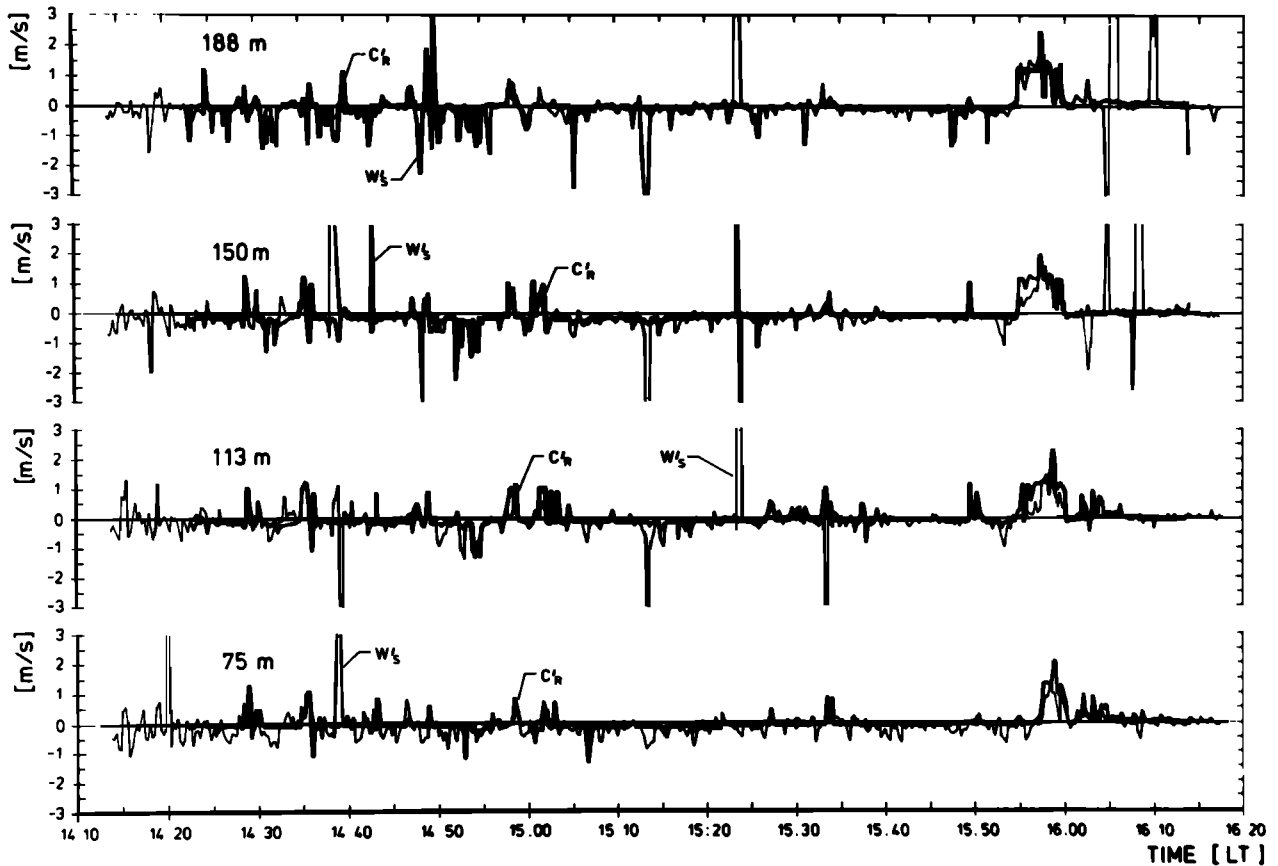


Fig. 4. Time series of RASS-derived sound velocity signal and sodar-derived vertical wind velocity signal at four altitudes. Sampling rate: 15 s.

and  $n$  is simply the number of samples as all samples of  $r_s$  are statistically independent.

#### MEASUREMENTS

We now report on a first attempt to employ these ideas, which was undertaken near Hamburg on the SW coast of the Elbe river on November 13, 1983. A RASS and sodar system as specified in Tables 1 and 2 had been put together at a horizontal distance of 15 m. According to the spatial and temporal resolution, horizontal homogeneity had been assumed between the corresponding measuring volumes of the systems. It was not clear in the beginning if the continuous sound source of the RASS eventually saturates the sodar receiver. But it turned out that no disturbing interference occurred.

The environmental temperature was about  $3^{\circ}\text{C}$  during the whole measuring period, and the prevailing wind direction was SE-parallel to the river.

Figure 4 shows time series of vertical wind  $w_s$  and sound velocity  $v_R$  at four measuring altitudes. The cutoff frequency due to volume averaging is

$$f_0 \approx U/\varphi z$$

where  $U$  is wind speed,  $\varphi$  the effective beam width, and  $z$  the measuring altitude.

The mean wind speed was about 3 m/s, resulting in a cutoff frequency of  $\frac{1}{4} \text{ s}^{-1}$  and  $\frac{1}{2} \text{ s}^{-1}$  for the sodar and RASS, respectively, in the lowest measuring altitude (75 m). Thus the pulse repetition frequency of  $\frac{1}{2} \text{ s}^{-1}$  of the sodar causes some aliasing which is, however, not considered further.

Each datum represents a 15-s average for both sodar and RASS. Thus also the minimum time lag increment  $\tau$  of the sampled covariance function is 15 s.

As the stratification was neutral, the characteristic period of the flux spectrum can be estimated according to (21). From this it follows that the condition of

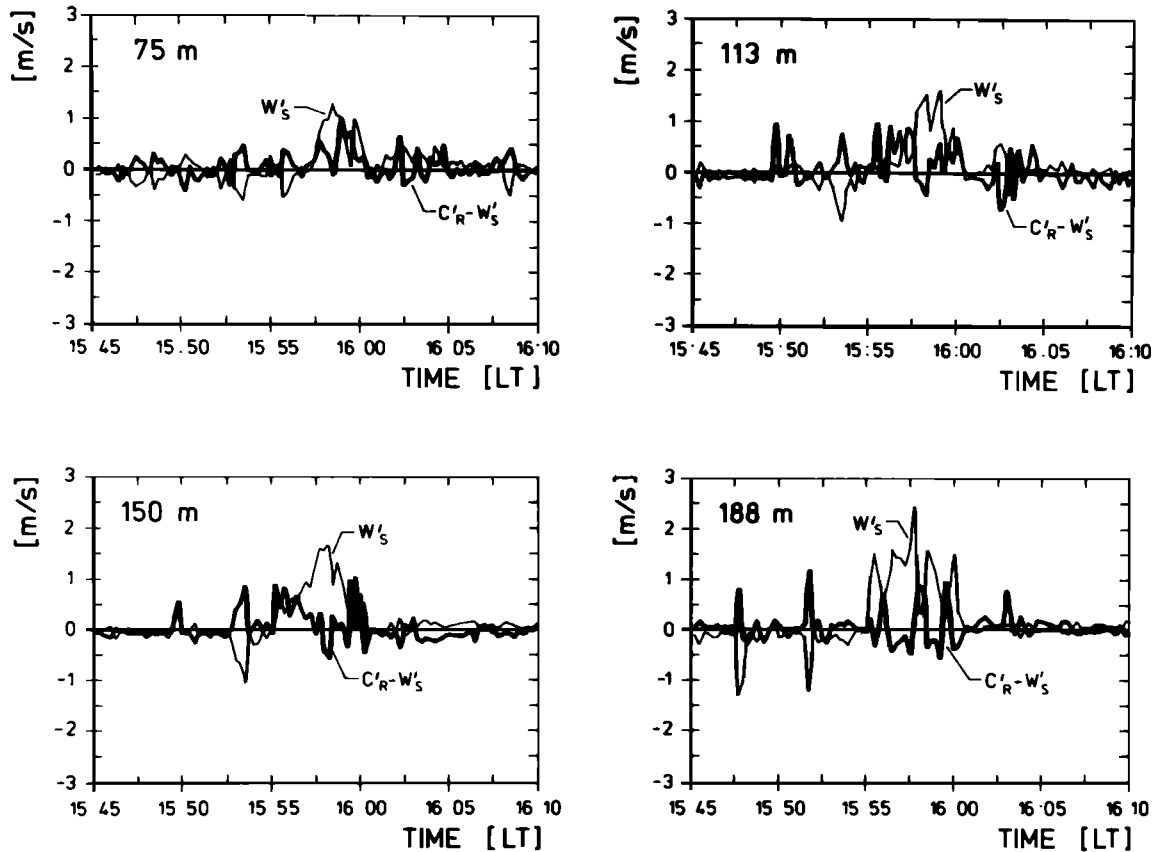


Fig. 5. Last 25 min as shown in Figure 4, but instead of the sound velocity signal  $v'_R$  the corrected quantity  $v'_R - w'_s$  is shown.

(22) is satisfied in all measuring altitudes and the interpolation according to (23) can be applied.

In order to estimate the heat flux profiles the time series of Figure 4 has been subdivided into 25-min intervals.

We generally expect the heat flux to be rather low with the exception of the last 25-min interval, when the wind turned from SE to NE, advecting warm air heated by the river. Figure 5 shows  $w'_s$  and  $v'_R - w'_s$  for this 25-min interval. The corresponding covariance functions are shown in Figure 6. One recognizes a sharp negative peak at zero time lag within a relatively broad structure. Qualitatively, this shape is to be expected from (20). The negative peak is attributed to  $\sigma^2(r_s)\delta(0, j)$ , and the broad structure is attributed to  $\langle w(i-j)c(i) \rangle$ . In this observation period there is obviously a time lag between the dominating wind and temperature excursions, which leads to a peak  $\langle w(i-j)c(i) \rangle$  at  $j \neq 0$ . No attempt has been made to explain this shift in terms of atmospheric processes.

The heat flux and its random error are estimated according to (23) and (31), respectively. In addition the standard deviation of the vertical wind component as measured with sodar and the random error of the vertical wind according to (32) have been determined. The quantities are given in Table 3.

TABLE 3. Heat Flux and Its Random Error and Standard Deviation and Random Error of the Vertical Wind Component as Measured by Sodar

| Measuring Height $h$ , m | Heat Flux $Q$ , W/m <sup>2</sup> | Estimated Random Error $\sigma(r_Q)$ , W/m <sup>2</sup> | Vertical Component Standard Deviation $\langle w_s^2 \rangle^{1/2}$ , m/s | Estimated Random Error $\sigma(r_s)$ , m/s |
|--------------------------|----------------------------------|---|---|--|
| 188                      | -20                              | $\pm 29$  | 0.52  | 0.27                                       |
| 150                      | 46                               | $\pm 12$  | 0.40  | 0.15                                       |
| 113                      | 39                               | $\pm 11$  | 0.37  | 0.14                                       |
| 75                       | 37                               | $\pm 5$   | 0.22  | 0.11                                       |



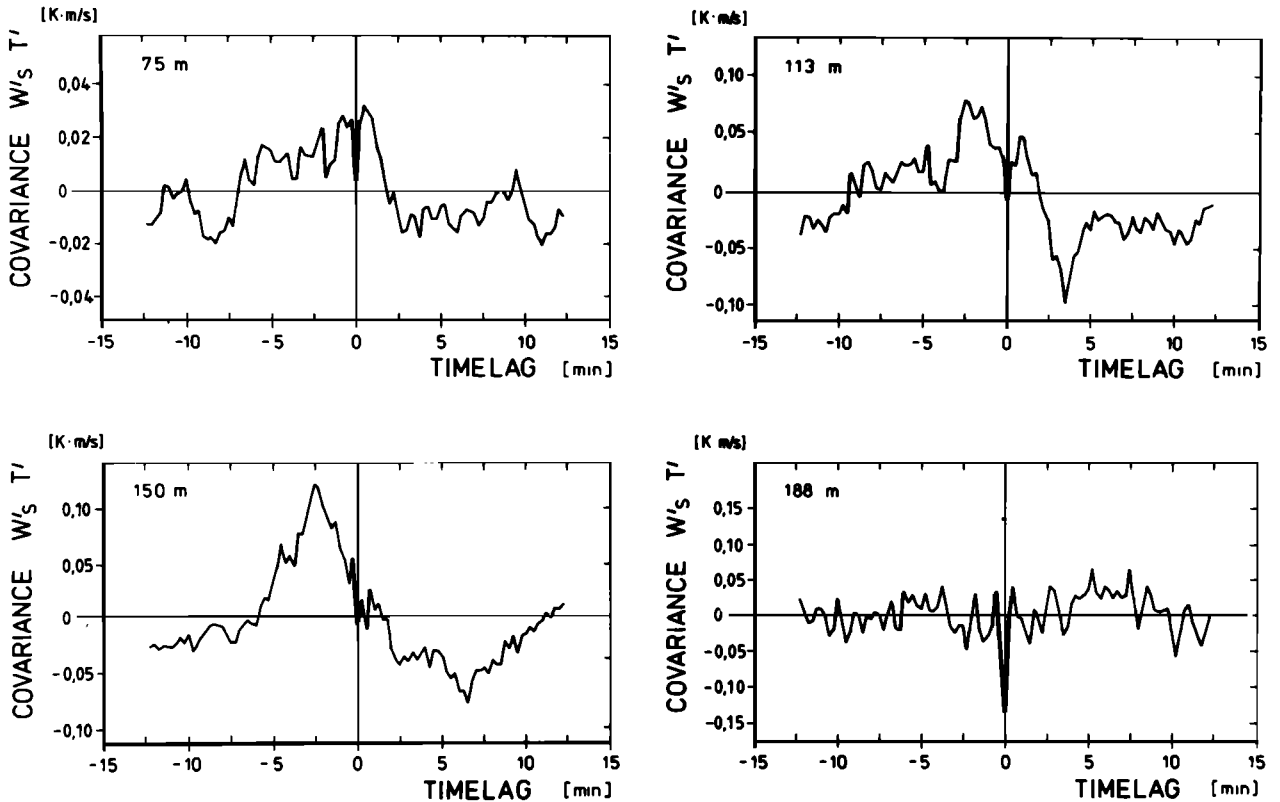


Fig. 6. Covariance function  $\langle w'T' \rangle$  for the last 25 min.

## CONCLUSION

The first measurement of heat flux by remote sensing has yielded plausible results in a situation of very weak convection. We conclude that measurements of heat flux by the eddy correlation method seem to be feasible in a combined operation of RASS and sodar. An easy algorithm has been developed to estimate the accuracy of the measurements, which at present depends mainly on the quality of the sodar data. In cases of strong convection a relative accuracy of  $\pm 20\%$  for the heat flux should be attainable.

We expect that the performance can be significantly improved if the sodar is replaced by an electromagnetic clear air radar having a sampling rate comparable to that of the RASS.

As a by-product the random error of high-resolution sodar-wind measurements has been determined experimentally.

*Acknowledgment.* We are grateful to D. Hasselmann for his helpful discussions during the preparation of this paper.

## REFERENCES

- Brown, E. H., and F. F. Hall, Jr., Advances in atmospheric acoustics, *Rev. Geophys.*, **16**, 47, 1978.
- Caughy, S. J., B. A. Crease, D. N. Asimakopoulos, and R. S. Cole, Quantitative bistatic acoustic soundings of the atmospheric boundary layer, *Q. J. R. Meteorol. Soc.*, **104**, 147, 1978.
- Frankel, M. S., and A. M. Peterson, Remote temperature profiling in the lower troposphere, *Radio Sci.*, **11**, 157, 1976.
- Harris, M. H., Absorption of sound in air versus humidity and temperature, *NASA Contract. Rep.*, CR-647, 1967.
- Jenkins, M. G., and D. G. Watts, *Spectral Analysis and Its Applications*, p. 337, Holden-Day, San Francisco, Calif., 1968.
- Kon, A. I., and V. I. Tatarskiy, The scattered signal frequency spectrum for radioacoustical atmospheric soundings, *Izv. Acad. Sci. USSR Atmos. Oceanic Phys.*, Engl. Transl., **16**, 142, 1980.
- Kon, A. I., A bistatic radioacoustic atmospheric sounding system, *Izv. Acad. Sci. USSR Atmos. Oceanic Phys.*, Engl. Transl., **17**, 481, 1981.
- Nalbandyan, O. G., The signal frequency spectrum in radioacoustic sounding of the atmosphere, *Izv. Acad. Sci. USSR Atmos. Oceanic Phys.*, Engl. Transl., **12**, 472, 1976a.
- Nalbandyan, O. G., Scattering of electromagnetic waves from a sound wave propagating in a turbulent atmosphere, *Izv. Acad. Sci. USSR Atmos. Oceanic Phys.*, Engl. Transl., **12**, 536, 1976b.

- Nalbandyan, O. G., The theory of radioacoustic sensing of the atmosphere, *Izv. Acad. Sci. USSR Atmos. Oceanic Phys.*, Engl. Transl., 13, 172, 1977.
- Panofsky, H. A., and E. Mares, Recent measurements of cospectra for heat flux and stress, *Q. J. R. Meteorol. Soc.*, 94, 581, 1968.
- Peters, G., H. Timmermann, and H. Hinzpeter, Temperature sounding in the planetary boundary layer by RASS—System analysis and results, *Int. J. Remote Sensing*, 4, 49, 1983.
- Peters, G., M. Latif, and W. J. Müller, Fluctuations of the vertical wind as measured by Doppler-SODAR, *Meteorol. Rundsch.*, 37, 16, 1984.
- Spizzichino, A., Discussion of the operating conditions of a Doppler sodar, *J. Geophys. Res.*, 79, 5585, 1974.
- Weill, A., C. Klapisz, B. Strauss, F. Baudin, C. Jaupart, P. van Grunderbeck, and J. P. Goutorbe, Measuring heat flux and structure functions of temperature fluctuations with an acoustic Doppler SODAR, *J. Appl. Meteorol.*, 19, 199, 1980.
- 
- G. Baumann, H. Hinzpeter, and G. Peters, Meteorological Institute, University Hamburg, Bundesstrasse 55, D-2000 Hamburg 13, Federal Republic of Germany.